ENERGY FUNCTION OPTIMIZATION FOR POWER SYSTEM PROTECTION ASSESSMENT

C. Singh
Dept. of Elec. & Comp. Eng.
The University of Newcastle
Callaghan NSW 2308 Australia

I.A. Hiskens
Dept. of Elec. & Comp. Eng.
University of Illinois at Urbana-Champaign
Urbana IL 61801 USA

Abstract

Following fault clearing, undesirable protection operation may play a role in weakening a power system. Such cascaded protection operation can lead to angle instability and/or voltage collapse. An energy function approach to assessing this protection operation was proposed in [7]. The critical energy used in the approach was given by a minimization problem. Unfortunately this minimization is difficult to solve due to its non-convex nature, and the presence of a large number of protection constraints. This paper develops several gradient-based optimization methods which display desirable convergence properties.

1 INTRODUCTION

Angle instability and voltage collapse are two important modes of system failure. Following fault clearing, undesirable protection operation may play a role in weakening a power system. For example, cascaded protection operation is a contributing factor in many cases of voltage collapse. Also, angle instability between generators frequently results in distance protection tripping feeders, which in turn may lead to system separation and islanding. Therefore there is value in the development of techniques for assessing whether a disturbance will initiate unwanted and often unmodelled protection action.

Transient energy function (TEF) methods have traditionally focussed on the assessment of angle instability [5]. Assessment of system behaviour is based on a comparison of the energy acquired during the disturbance with a critical value of energy. This critical energy provides an estimate of the boundary of the stability region. A similar approach can now be used to assess voltage collapse with recent developments in energy functions [3] which allow load dynamics to be modelled.

However, modifications are required to incorporate protection operation into TEF methods. This revolves around a new procedure for calculating the critical energy. Rather than the critical energy reflecting the stability boundary, it must now provide an estimate of the conditions under which protection operation would occur. The first step in determining this critical energy is to define mathematically the protection surface, i.e., the set of points in state space at which the protection relay will operate. The critical energy is then the amount of energy that could be acquired by the system such that the post-fault trajectory was tangential to the protection surface. Acquisition of a larger amount of energy could result in the system trajectory encountering the protection surface, and hence protection operation. Protection would not operate if the system acquired less energy.

In [7], this critical energy was found as the solution of a constrained minimization problem. An overview is given in Section 3. Unfortunately the minimization is difficult to solve due to the non-convex nature of the cost function and constraints. This is especially so for power systems which contain a large number of protection relays, i.e., actual power systems. Non-traditional optimization techniques such as simulated annealing [8] have been used to solve this problem. However, they are often slow. Several gradient-based optimization methods display more desirable convergence properties. This paper developes those methods.

2 MODELS

2.1 Power System Model

Rigorous development of direct protection assessment concepts requires the use of a strict Lyapunov

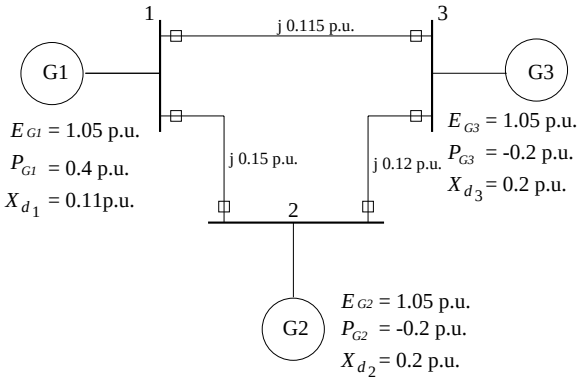

Figure 1: 3-Machine 3-Bus system.

energy function. For this, generators are modelled using the classical machine model, active loads are considered to be constant and reactive power loads are modelled using either a static voltage dependent or dynamic load model [3]. Under these assumptions, the power system model can be written in a general differential-algebraic (DA) form

$$\dot{x} = f(x,y) \quad (1)$$
$$0 = g(x,y) \quad (2)$$

where $x = [\omega^t\ \delta^t\ x_q^t]^t$; ω is a m-vector of generator speeds; δ is a $(m-1)$-vector of generator angles; x_q is the d-vector of dynamic load states; and y is the $2n$-vector of algebraic variables, i.e., load bus voltage magnitudes and angles. (Superscript 't' denotes matrix transpose). It will be assumed throughout that Jacobian $\frac{\partial g}{\partial y}$ is nonsingular, i.e., solutions of $g = 0$ are well defined.

Exact details of model and energy function development can be found in [3]. The corresponding energy function has the form

$$V(\omega_g, \delta, x_q, v) = V_{KE}(\omega_g) + V_{PE}(\delta, x_q, v) \quad (3)$$

where V_{KE} and V_{PE} can be thought of as kinetic and potential energy terms respectively. Contours of potential energy (PE) for the simple unloaded system of Figure 1 are shown in Figure 2 (dark lines).

2.2 Protection Model

This paper considers distance protection relays [1], though the concepts extend to any constraints which restrict system behaviour to a region of state space. Distance protection relays monitor the apparent impedance seen from a bus, and operate if that impedance enters the trip region. The operating criterion can be written in the general form

$$H_{ik}(y) \leq 0. \quad (4)$$

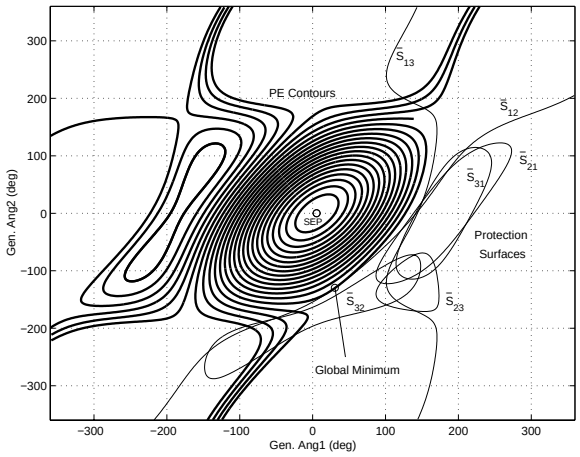

Figure 2: State Space View of Potential Energy Contours and Protection Surfaces.

Full details of the relationship between (4) and typical mho characteristics can be found in [6].

It is convenient to define each protection operating region by the set

$$S_{ik} = \{(x,y) \mid H_{ik}(y) \leq 0\}. \quad (5)$$

Its boundary $\bar{S}_{ik}$ is given by $H_{ik}(y) = 0$, and shall be referred to as the *protection surface*. As an example, a state space view of all protection surfaces $\bar{S}_{ik}$, $i = 1, \cdots, 3$, $k = 1, \cdots, 3$, corresponding to zone 3 are depicted in Figure 2 for the system of Figure 1.

3 PROBLEM FORMULATION

The value of critical energy required for assessment of protection operation is given by minimizing potential energy over all protection surfaces, i.e.,

$$\min_{(x,y) \in S} \quad V_{PE}(x,y) \quad (6)$$
$$\text{s.t.} \quad g(x,y) = 0 \quad (7)$$

where

$$S = \bigcup_{i,k} S_{ik}. \quad (8)$$

Figure 2 shows the solution of this optimization problem for the example 3-machine 3-bus system. The global minimum for the protection constraints occurs at (30.62, -129.83), with potential energy equal to 5.55. It was shown in [7] that if the fault was cleared with this critical energy, then the system trajectory never encountered the protection surfaces, and hence system integrity was maintained without any cascaded protection action. However, note from Figure 2 that the potential energy function and protection constraints

are quite non-convex, posing substantial difficulty in determining the local minimum of interest.

Simulated annealing algorithms were proposed in [8] to locate the global minimum. However those algorithms are not preferable for the following two reasons: (i) the global minimum is not always the local minimum of interest, possibly resulting in conservative stability assessment; and (ii) they are often slow. A more efficient way of locating the local minimum is required. This paper proposes gradient-based algorithms which demonstrate better convergence results. They make use of Lagrangian multiplier theory [2].

It has been observed that following a fault, only certain relays on certain lines are likely to operate. The rest of the relays are not relevant to that disturbance, and should not be included in calculating the critical energy. The relays that may operate are called *controlling relays*, whilst the relay which ultimately operates first will be referred to as the *critical relay*.

Suppose the most critical relay for the given fault has been found [4, 6]. This implies that we need consider only the single protection constraint corresponding to that relay. Using Lagrangian multiplier theory, the constrained minimization problem (6)-(7) can be transformed into locating the unconstrained minimum of the Lagrangian function $L : \Re^{m+d+4n} \longmapsto \Re$ defined as

$$L(x, y, \lambda, \mu) = V_{PE}(x, y) + \sum_{i=1}^{2n} \lambda_i g_i(x, y) + \mu H_{ik}(y) \tag{9}$$

where λ is a $2n$-dimensional (column) vector of Lagrangian multipliers associated with constraints g, and μ is the the Lagrangian multiplier associated with the protection constraint H_{ik}. (Note that in (9), x only includes δ and x_q). The minimum of L is given by the first order optimality conditions [2]. If $(x^*, y^*, \lambda^*, \mu^*)$ is a local minimum of function L, then first order optimal conditions can be written as

$$\nabla_{x,y,\lambda,\mu} L(x^*, y^*, \lambda^*, \mu^*) = 0. \tag{10}$$

The first order optimal conditions (10) represent $m+d+4n$ equations in $m+d+4n$ unknowns, viz., the states x, y and the Lagrangian multipliers λ and μ. Equation (10) can be written explicitly as

$$\begin{aligned} \nabla_x V_{PE} + g_x^t \lambda &= 0 && (11)\\ g_y^t \lambda + \mu \nabla_y H_{ik}(y) &= 0 && (12)\\ g(x, y) &= 0 && (13)\\ H_{ik}(y) &= 0 && (14) \end{aligned}$$

where $g_x \equiv \frac{\partial g}{\partial x}$, and other partial derivatives follow the same convention. Equations (11)-(14) also make use of the facts that $H_{ik}(y)$ is not a function of x, and $\nabla_y V_{PE}(x, y) = g(x, y) = 0$ at all solution points [5]. They form a fully determined set of equations, and can be solved simultaneously to give local minima $(x^*, y^*, \lambda^*, \mu^*)$. Note that multiple solutions may exist. Special care should be exercised in determining the local minimum of interest.

4 GRADIENT-BASED ALGORITHMS

4.1 Background

The Newton-Raphson algorithm can be used to solve the system of equations (11)-(14). The advantage of using this gradient-based algorithm over simulated annealing algorithms is that if a good initial guess is known, then Newton-Raphson takes only a few iterations to converge. Writing (11)-(14) as

$$F(z) = 0$$

where $z = [x^t \ y^t \ \lambda^t \ \mu]^t$, the Newton-Raphson algorithm uses the iterative process

$$z^{k+1} = z^k - \alpha^k \, J^{-1}(z^k) F(z^k) \tag{15}$$

to move from the k^{th} to the $(k+1)^{th}$ iteration. In (15), α is the stepsize (accelaration factor) and J is the Jacobian matrix of the system (11)-(14) calculated at the k^{th} iteration. J is also the Hessian matrix of the Lagrangian function L [2].

Unfortunately the Newton-Raphson algorithm suffers from the major disadvantage of requiring a good initial guess. For the example system in Figure 1, the state space is only 2-dimensional and a good guess of the initial point is possible from the geometry of the cost function V_{PE} and the protection surfaces; see Figure 2. However the state space of practical power systems has high dimension, so visualization becomes impossible.

The difficulty of finding a good initial guess is compounded by the presence of Lagrangian multipliers, which introduce $2n+1$ extra variables. To ensure convergence, it is desirable that the initial guess is close to the optimal solution, or at least some of the equations (11)-(14) are satisfied. The stable equilibrium point (SEP) often provides a suitable initial guess. The advantage of using the SEP as the initial guess is that $\nabla_x V_{PE}$ is zero and $g = 0$, i.e., $2n$ of the $m+d+4n$ equations are satisfied.

Several approaches have been adopted to implement (15) using the SEP as the initial guess. They are now discussed.

4.2 One Step Approach

The one step algorithm starts from the SEP and follows a sequence of points produced by (15) that (hopefully) converge to the optimum solution. One approach is to use a *constant* stepsize, with very small initial values for λ and μ. Unfortunately, (15) diverges if the stepsize is too big. Testing has shown that convergence can usually be obtained for α in the range $0 < \alpha < 1$. However, the choice of α is crucial. Different stepsizes can result in convergence to different local minima. Also, if α is too small, the convergence rate is quite slow, especially when approaching the optimum solution. This is because the gradient F of the Lagrangian function L vanishes and the improvement in the cost reduces as the optimum solution point is approached.

The convergence rate can be improved by using a *variable* stepsize. Initially $0 < \alpha < 1$, then α is increased as the optimum solution is approached. Simulations indicate that this *variable* stepsize algorithm converges 2-3 times faster than the *constant* stepsize version. The final value of α can be up to 10 times the initial value.

It should be noted though that the success of both the *constant* and *variable* stepsize approaches depends of the choice of initial α. Unfortunately, there is no systematic way of determining that initial value, so their application is limited. Hence these one step approaches will not be discussed further.

4.3 Two Step Approach

The SEP is often remote from the desired solution of (11)-(14). Therefore a better initial guess is needed for reliable convergence of (15). To achieve this, a two step approach is proposed. The *first step* of the algorithm finds a point that is closer to the optimum solution. In the *second step*, (11)-(14) are solved, starting from the initial point obtained in the first step.

The function $H_{ik}(y)$ is directly related to the apparent impedance [6]. Therefore at the SEP, $H_{ik}(y) > 0$. Movement from the SEP towards the protection operating characteristic corresponds to a reduction in $H_{ik}(y)$. (Recall that at the operating characteristic, $H_{ik}(y) = 0$.) The direction in which $H_{ik}(y)$ reduces fastest generally indicates the region of state space where protection operation is most likely to occur.

Therefore the first step of the two step approach begins at the SEP and minimizes $H_{ik}(y)$ along the steepest decent direction until $H_{ik}(y) = 0$. From (2), it can be seen that y is an implicit function of x, so we can define $H_{ik}(y(x)) \equiv \bar{H}_{ik}(x)$. Then

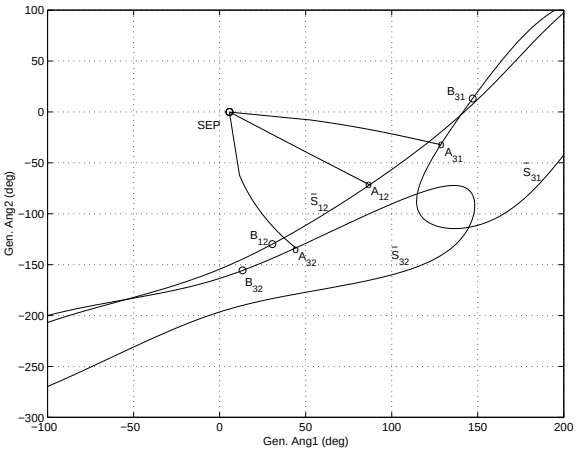

Figure 3: Two Step Approach Lands Close to the Optimum Solution.

points along the steepest decent direction are given by

$$x^{k+1} = x^k - \alpha^k \nabla_x \bar{H}_{ik}(x^k) \tag{16}$$

with (2) satisfied at each point. The total derivative of (2) allows (16) to be rewritten as

$$x^{k+1} = x^k + \alpha^k \nabla_y H_{ik}(y)^t g_y^{-1} g_x. \tag{17}$$

The algorithm (17) moves in the steepest descent direction of $H_{ik}(y)$, and will continue until $H_{ik}(y) = 0$. If the function $H_{ik}(y)$ is convex, at least near the SEP, and has a nice shape in state space, then the final point of the first step will be close to the optimum solution. It can be used as the initial guess in the second step to solve the original optimization (11)-(14). Note that another advantage of using this point is that both (13) and (14) are satisfied.

Implementation of the two step approach is illustrated in Figure 3 for the three protection surfaces $\bar{S}_{12}$, $\bar{S}_{31}$ and $\bar{S}_{32}$. Points A_{ik} are end points of the first step, and B_{ik} are the optimum solutions lying on the corresponding protection surfaces $\bar{S}_{ik}$. Note that points A_{31} and A_{32} are close to the corresponding optimum points B_{31} and B_{32}. The Newton-Raphson algorithm (15) gave fast convergence in these cases.

It should be mentioned that the Lagrangian multipliers also play a significant role in the minimization of the Lagrangian function L. In fact the algorithm may diverge if poor initial guesses of λ and μ are used, even if x and y are at the exact optimum solution. The following section addresses the issue of Lagrangian multipliers in more detail, and proposes several ways to compute them.

4.4 Computation of Lagrangian Multipliers

Section 4.3 presented techniques for obtaining initial guesses of x and y that are close to the optimum solution. However to efficiently carry out the minimization of the Lagrangian function L, it is also important to reduce the uncertainty in the initial guesses of the Lagrangian multipliers λ and μ. This can be achieved either by eliminating (at least partially) λ and μ from the original problem, or computing them systematically. Both approaches are now considered.

4.4.1 Partial Elimination of Lagrangian Multipliers

Partial elimination of Lagrangian multipliers in the given optimization problem follows from the relationship between λ and μ given by (12). Simple manipulation yields

$$\lambda = -\mu g_y^{t^{-1}} \nabla_y H_{ik}, \tag{18}$$

i.e., at any point where (12) is satisfied, λ can be calculated by specifying μ only. Note that in the two step approach, (13) and (14) are satisfied at the end of the first step. Also, if the end point is sufficiently close to the optimum solution, for example A_{31} and A_{32} in Figure 3, it is reasonable to assume that (11) and (12) are approximately satisfied, i.e.,

$$g_y^t \lambda + \mu \nabla_y H_{ik} \approx 0 \tag{19}$$

and hence λ can be calculated from (18) by specifying just one multiplier μ. This greatly reduces the uncertainty in the initial guess of Lagrangian multipliers.

The above approximation can be demonstrated for $\bar{S}_{32}$. First note that the actual values of μ and λ at the optimum solution point B_{32} are $\mu^* = 2.502$ and

$$\lambda^* = [0.054 \;\; -0.303 \;\; 0.083 \;\; 0.138 \;\; 1.053 \;\; 0.115]^t.$$

Assume for now that μ^* is known. Then λ^* can be approximated using (18) to give

$$\lambda^*_{approx} = [0.092 \;\; -0.343 \;\; 0.097 \;\; 0.130 \;\; 1.098 \;\; 0.122]^t,$$

which is quite close to λ^*.

4.4.2 Quadratic Approximation of μ

In Section 4.4.1, μ^* was used to find an approximate λ^*. However μ^* is usually not known. An approach is now proposed for finding an approximate value for μ^* near the optimum solution. That estimate can then be used to obtain λ^*_{approx}.

By substituting λ from (18) into (11), we have

$$\nabla_x V_{PE} - \mu (g_y^{-1} g_x)^t \nabla_y H_{ik} = 0. \tag{20}$$

Equation (20) is approximately satisfied at the end point of the first step in the two step approach. An approximate value of μ^* is given by the value of μ which minimizes the difference between the LHS and RHS of (20), calculated at the end point. Define

$$Q = \nabla_x V_{PE} - \mu (g_y^{-1} g_x)^t \nabla_y H_{ik}.$$

The appropriate value of μ can be found by solving the quadratic optimization problem

$$\min_{\mu} Q^t Q. \tag{21}$$

The solution of (21) is given by $\nabla_\mu \, Q^t Q = 0$, which results in

$$\mu^*_{approx} = \frac{\sum_{i=1}^{m+d-1} \nabla_{x_i} V_{PE} \, p_i}{\sum_{i=1}^{m+d-1} p_i^2} \tag{22}$$

where $p = (g_y^{-1} g_x)^t \nabla_y H_{ik}$. For the previous example based on $\bar{S}_{32}$, (22) gave $\mu^*_{approx} = 2.218$, which is very close to the actual $\mu^* = 2.502$. Once μ^*_{approx} is known, λ^*_{approx} can easily be found using (18).

4.4.3 Successive Computation of Lagrangian Multipliers

In the two step approach, partial elimination of λ along with quadratic approximation of μ works well if the point at the end of the first step is close to the optimum solution, i.e., if assumption (19) holds. However, that is not always the case, as shown by surface $\bar{S}_{12}$ in Figure 3. In badly behaved cases, the two step approach fails to give a good initial guess of the states x and y, and the Lagrangian multipliers λ and μ. To overcome these difficulties, a more robust continuation-type algorithm, which successively computes the Lagrangian multipliers, has been developed.

As mentioned in Section 4.3, $H_{ik}(y_{sep}) > 0$ at the SEP. Let $H_{ik}(y_{sep}) = \theta_{sep}$. Also recall that $H_{ik}(y) = 0$ on the protection surface. Therefore the desired minimization can be achieved by solving

$$\nabla_x V_{PE} + g_x^t \lambda = 0 \tag{23}$$

$$g_y^t \lambda + \mu \nabla_y H_{ik}(y) = 0 \tag{24}$$

$$g(x, y) = 0 \tag{25}$$

$$H_{ik}(y) - \theta = 0 \tag{26}$$

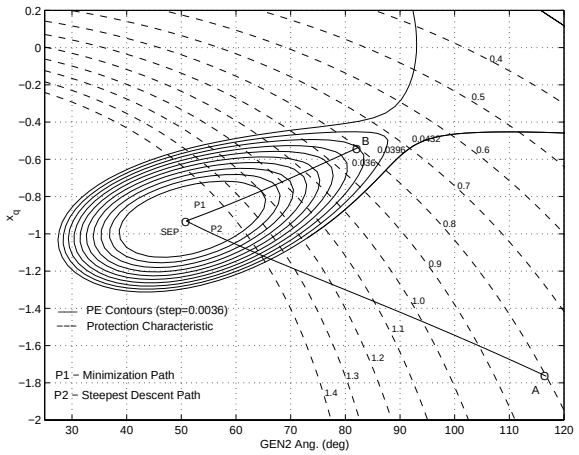

Figure 4: Illustration of Successive Computation of Lagrangian Multipliers.

for a sequence of values of θ from θ_{sep} to 0. Note that $\nabla_x V_{PE} = 0$ at the SEP. So when $\theta = \theta_{sep}$, (23)-(26) are trivially satisfied by $\lambda = 0$ and $\mu = 0$.

Each step along the path from the SEP to the desired minimum consists of two parts. Consider the step from θ_l to θ_{l+1}. Initially a steepest descent direction is followed from the minimum point on $H_{ik}(y) = \theta_l$ to a point on $H_{ik}(y) = \theta_{l+1}$. This is similar to the first step in the two step approach given in Section 4.3. The minimization (23)-(26) is then solved for this new protection constraint. The initial guess of all variables at each step is available from the solution of the previous step. This process is continued until $\theta = 0$, when the minimization gives the desired value of critical energy.

The successive computation algorithm has been successfully applied to minimization over all the individual protection characteristics of the system in Figure 1. But for clearer illustration, in this case we shall use the 2-machine 1-dynamic load example given in [3]. Minimization over the most critical protection surface S_{32} is illustrated in Figure 4. (The minimum potential energy is 0.036, which occurs at the point $(\delta_{g2}, x_q) = (82.1^o, -0.57)$.) The path P1 leads to the required minimum point. The algorithm terminates when the path encounteres the desired protection constraint.

The successive computation algorithm has been found to be the most robust of all the gradient-based and simulated annealing algorithms. Unfortunately the computational cost can very high if small steps in θ are required. However, speed can be improved using sparse matrix techniques and by avoiding inversion of the Jacobian J at every step.

5 CONCLUSIONS

Locating the correct local minimum is crucial in calculating the critical energy for energy function assessment of protection operation. This is a difficult minimization problem. Lagrangian multiplier theory is used in this paper to motivate some gradient-based algorithms. These techniques exhibit better convergence properties than the simulated annealing algorithms given in [8].

The gradient-based algorithms require a good initial guess of all problem variables to ensure convergence. Several approaches have been presented for obtaining a good initial guess of the states x and y. Also, techniques have been proposed and illustrated for the efficient estimation of initial values of the Lagrangian multipliers λ and μ. Examples have been used to illustrate the advantages and shortcomings of the various algorithms.

References

[1] A. R. Bergen. *Power System Analysis.* Prentice-Hall, Englewood Cliffs, NJ, 1986.

[2] D. P. Bertsekas. *Nonlinear Programming.* Athena Scientific, Belmont, MA, 1995.

[3] R. J. Davy and I. A. Hiskens. Lyapunov functions for multi-machine power systems with dynamic loads. *IEEE Transactions on Circuits and Systems-I*, 44(9):796–812, September 1997.

[4] F. Dobraca, M. A. Pai, and P. W. Sauer. Relay margins as a tool for dynamical security analysis. *International Journal of Electrical Power and Energy Systems*, 12(4):226–234, October 1990.

[5] M. A. Pai. *Energy Function Analysis For Power System Stability.* Kluwer Academic Publishers, Boston, 1989.

[6] C. Singh and I. A. Hiskens. Direct assessment of vulnerability to protection operation. *IEEE Transactions on Power Systems*, Submitted for publication.

[7] C. Singh and I. A. Hiskens. Energy function assessment of protection operation. *Proceedings of the Australasian Universities Power Engineering Conference*, Hobart, Australia, September 1998.

[8] C. Singh, I. A. Hiskens, and P. R. Kumar. Application of simulated annealing to power system protection assessment. *Proceedings of the 37th Conference on Decision and Control*, Tempa, Florida, December, 1998.